Probing the Sources of Uncertainty in Transient Warming on Different Time-Scales

Nicholas J. Lutsko[1]

[1]Department of Earth, Atmospheric, and Planetary Sciences, Massachusetts Institute of Technology, Cambridge, Massachusetts.

Max Popp[2]

[2]Laboratoire de Météorologique Dynamique, Sorbonne Université, Ecole Normale Supérieure, Ecole Polytechnique, Paris, France.

Key Points:

- Transient warming is most sensitive to uncertainty in the radiative forcing and not to uncertainty in the radiative feedbacks.
- Reducing uncertainty in the radiative forcing is the most efficient way of reducing uncertainty in transient climate response
- Radiative feedbacks of climate models that are tuned to the historical record are highly sensitive to the assumed historical forcing.

Corresponding author: Nicholas Lutsko, `lutsko@mit.edu`

Abstract

The rate of transient warming is determined by a number of factors, notably the radiative forcing from increasing CO_2 concentrations and the net radiative feedback. Uncertainty in transient warming comes from both the uncertainty in each factor and from the warming's sensitivity to uncertainty in each factor. An energy balance model is used to untangle these two components of uncertainty in transient warming, which is shown to be most sensitive to uncertainty in the forcing and not to uncertainty in radiative feedbacks. Additionally, uncertainty in the efficacy of ocean heat uptake is more important than uncertainty in the rate of ocean heat uptake. Three further implications are: (1) transient warming is highly sensitive to uncertainty in emissions; (2) caution is warranted when extrapolating future warming trends from short-lived climate perturbations; and (3) climate models tuned using the historical record are highly sensitive to assumptions made about the historical forcing.

1 Introduction

Predicting the warming of global-mean surface temperature in response to increased CO_2 concentrations is one of the central goals of climate science. A convenient and effective way of quantifying future warming is through climate sensitivity, which can be defined in several ways. The equilibrium climate sensitivity (ECS) is the equilibrated response of global-mean surface temperature to a doubling of CO_2 concentrations, and is equal to the forcing due to doubling CO_2 (F) divided by the net radiative feedback which brings the system back into equilibrium (λ):

$$ECS = F/\lambda. \tag{1}$$

The ECS is a measure of the equilibrium state of the climate system, however anthropogenic climate change is a transient perturbation. A useful metric of transient warming is the transient climate response (TCR): the response of global-mean surface temperature after 70 years of increasing CO_2 concentrations by 1% per year (i.e., after CO_2 concentrations have doubled). The TCR can be scaled for a given emission scenario, and provides an estimate of future warming on a timescale at which human action is possible to limit or mitigate further warming. Recently the closely related T140, the warming after 140 years of increasing CO_2 concentrations by 1% per year, has also been used to quantify the difference in transient warming after one doubling compared to after two doublings of CO_2 concentrations (*Gregory et al.* [2015]; *Grose et al.* [2018]).

Large uncertainties in these measures of Earth's climate sensitivity persist, with the IPCC AR5 report giving "likely" ranges of 2.5-4.5K for the ECS and 1.0-2.5K for the TCR [*Stocker*, 2013], limiting our ability to predict future warming. Much effort has gone into reducing these uncertainties, with little effect. We argue here that progress in narrowing these uncertainty ranges can be made by focusing more carefully on the sources of uncertainty in each of these metrics. Specifically, uncertainty in a given metric can be decomposed into two components: *(1)* the uncertainty in each factor which determines that metric, and *(2)* the sensitivity of the metric to uncertainty in each factor [*Hamby*, 1994]. This second component of uncertainty has received little attention from the climate sensitivity community, as the focus has been on constraining the most uncertain factors. However, a factor may be highly uncertainty but contribute little to uncertainty; conversely, identifying the factors to which future warming is most sensitive can reveal the most promising paths for narrowing the uncertainty in Earth's climate sensitivity.

In the case of the ECS, equation 1 makes clear that the uncertainty is due to the relative uncertainties in F and in λ^{-1}. The small number of factors responsible for uncertainty in the ECS comes from the steady-state definition of ECS, so that there are no time-dependent factors. Uncertainties in λ^{-1} and F are linearly related to uncertainty in the ECS, and the larger relative uncertainty in λ^{-1} (Figure 1a) justifies the intense focus in the climate science community on better constraining the net radiative feedback.

By contrast, the uncertainty in transient warming (quantified by TCR, T140 or any other metric of transient warming) is determined by several factors, including the radiative forcing that causes the climate response, the radiative feedbacks which ultimately bring the climate system back to equilibrium and the rate at which heat is transferred from the surface ocean to the deep ocean (*Gregory* [2000]; *Dufresne and Bony* [2008]; *Held et al.* [2010]; *Geoffroy et al.* [2012]). In this study, we analyze a widely used two-box energy balance model (EBM) of Earth's climate system to quantify the sensitivity of transient warming to uncertainty in each of these factors as a function of time-scale. Our analysis includes both theoretical considerations (section 2) and analysis of data from a set of models participating in the Fifth Climate Model Intercomparison Project (CMIP5, section 3).

Both analyses demonstrate that, even after 140 years, transient warming is most sensitive to uncertainty in the radiative forcing and not, as is often assumed implicitly, to sensitivity in the radiative feedbacks. This implies that the most effective way of reducing uncertainty in transient warming is to reduce uncertainty in the radiative forcing, rather than focusing on the radiative feedbacks. In other words, reducing the relative uncertainty in F by 1% would reduce the uncertainties in the TCR and the T140 substantially more than reducing the relative uncertainty in λ by 1%.

Our results have several other important implications. First, transient warming is highly sensitive to uncertainties in the carbon cycle feedbacks which determine the fraction of emitted CO_2 that is removed from the atmosphere. For this reason, uncertainty in future emissions can easily overwhelm uncertainties in the climate system's radiative feedbacks. Second, the changing contributions of the various factors to uncertainty on different time-scales suggest caution when extrapolating the climate system's response to short-term perturbations, such as volcanic eruptions, to sustained climate perturbations, such as long-term CO_2 increases. Finally, our results imply that the radiative feedbacks in models that are "tuned" by fitting to the historical record are strongly controlled by the assumed historical forcing. As increasing numbers of models include a representation of the aerosol indirect effect, which increases the spread in the assumed historical forcing, this suggests that the intermodel spread in the net radiative feedback will be substantially larger in the next generation of climate models.

2 Theoretical Analysis of a Two-Box EBM

In order to evaluate the causes of uncertainty in transient warming, we analyze a widely used EBM consisting of two boxes, one representing the combined land surface and ocean mixed-layer and the other representing the deep ocean (*Gregory* [2000]; *Held et al.* [2010]; *Geoffroy et al.* [2013a]; *Geoffroy et al.* [2013b]; *Gregory et al.* [2015]). This EBM can reproduce the evolution of climate models' global-mean surface temperature in simulations in which CO_2 is either instantaneously doubled or in which CO_2 is increased by 1% per year (Supplemental Figure 1), and is written as:

$$c\frac{dT_1(t)}{dt} = \Delta F(t) - \lambda T_1(t) - \epsilon\gamma(T_1(t) - T_2(t)), \tag{2}$$

$$c_0\frac{dT_2(t)}{dt} = \gamma(T_1(t) - T_2(t)), \tag{3}$$

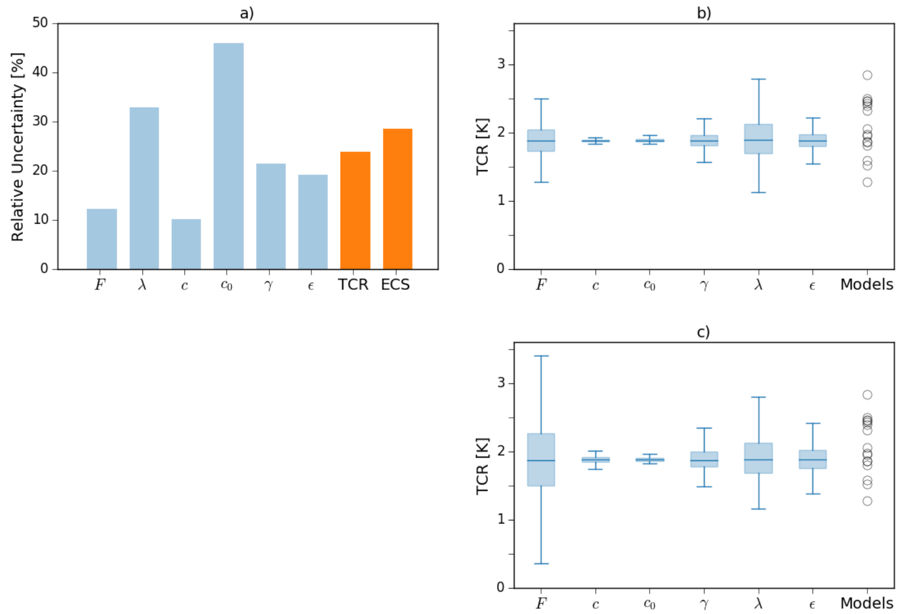

Figure 1. a) The relative uncertainties in the six parameters of the EBM (blue bars), based on fitting the EBM to the 18 CMIP5 models, as well as the uncertainties in the ECS and the TCR (orange bars). b) Box-and-whisker plots showing the distributions of TCR from the initial EBM integrations. The boxes show ±one standard deviation, the horizontal lines show the mean and the whiskers denote ±two standard deviations. The round markers show the models' TCRs. c) Same as panel b) but the EBM integrations are performed assuming the same relative uncertainty in each parameter.

with c the heat capacity of the surface box, T_1 the surface temperature anomaly, λ the net radiative feedback, ϵ the efficacy of ocean heat uptake, γ the rate of heat exchange between the surface and deep ocean, T_2 the temperature anomaly of the deep ocean and c_0 the heat capacity of the deep ocean. The efficacy term was first proposed by *Winton et al.* [2010] as a means of accounting for the fact that the sensitivity of transient warming to ocean heat uptake differs from the sensitivity to radiative forcing. Including ϵ allows the EBM to capture the time-dependence of the climate feedback and ocean heat uptake seen in climate model simulations.

ΔF is the radiative forcing due to increasing CO_2 concentrations at time t, which can be approximated as $\Delta F(t) = F \ln(C(t)/C_0)$ (*Myhre et al.* [1998]; *Etminan et al.* [2016]), with $C(t)$ the carbon dioxide concentration at time t and C_0 the pre-industrial atmospheric concentration of CO_2. For a 1% per year increase in atmospheric CO_2 concentrations this leads to

$$\Delta F(t) \approx \frac{Ft}{70\text{years}}. \tag{4}$$

The TCR is equal to T_1 after 70 years of increasing CO_2 concentrations by 1% per year and T140 is equal to T_1 after 140 years of increasing CO_2. In equilibrium the derivatives of T_1 and T_2 vanish and it can be readily verified that the ECS= F/λ.

Using this approximation for the forcing, the EBM can be solved for T_1 and T_2 (*Geoffroy et al.* [2013a]) to give

$$T_1 = \frac{F}{70\lambda}\left[t - \tau_f a_f(1 - e^{-t/\tau_f}) - \tau_s a_s(1 - e^{-t/\tau_s})\right], \tag{5}$$

$$T_2 = \frac{F}{70\lambda}\left[t - \phi_f \tau_f a_f(1 - e^{-t/\tau_f}) - \phi_s \tau_s a_s(1 - e^{-t/\tau_s})\right], \tag{6}$$

where τ_f and τ_s are the time-scales of a fast mode of response and a slow mode of response, respectively, and a_f and a_s are the contributions of the fast and slow modes to the heat uptake temperature $T_H(t) = ECS - T_1(t)$. Expressions for the τs and the as are given in Supplemental Table 1.

Apart from the linear dependence on F, the relationships between uncertainty in the other five free parameters in the EBM (λ, γ, ϵ, c and c_0) and uncertainty in transient warming are opaque in this setting. More simply, the EBM can be transformed to frequency space and solved for T_1, giving:

$$\hat{T}_1 = \frac{\omega}{70} \times \frac{F}{\lambda + ic\omega + \epsilon\gamma\left(1 - \gamma/(ic_0\omega + \gamma)\right)}, \tag{7}$$

where the overhat denotes a Fourier transform, ω is frequency and we assume that the six co-efficients are independent of frequency. ω is the inverse of the period P, so that low frequencies (small ω) correspond to long time-scales, and vice-versa. The absolute value of $\hat{T}_1$ is

$$|\hat{T}_1| \approx \frac{\omega F}{70} \times \sqrt{\frac{1}{\left[\lambda + \epsilon\gamma\left(1 - \frac{\gamma^2}{\gamma^2 + c_0^2\omega^2}\right)\right]^2 + \omega^2 c^2 + \frac{2\omega c c_0 \epsilon}{\gamma^2 + c_0^2\omega^2} + c_0^2\omega^2\epsilon^2/(\gamma^2 + c_0^2\omega^2)^2}}, \tag{8}$$

where a strong dependence of $|\hat{T}_1|$ on one of the six variables means that uncertainty in that variable has a large impact on the uncertainty of $|\hat{T}_1|$. For instance, the linear relationship with F means that transient warming is sensitive to uncertainty in F on all time-scales.

Although it may appear complicated, equation 8 simplifies on different time-scales, allowing the differing contributions of λ, γ, ϵ, c and c_0 to uncertainty in transient warming on these time-scales to be understood. First, we define “long" times-scales as $\omega \leq$

$\gamma/c_0 := \omega_L$, or $t > P_L = c_0/\gamma$. The time-scale P_L is the time-scale at which the deep ocean equilibrates. For time-scales much shorter than this, when $\omega >> \omega_L$ (or $t << P_L$) the expression for $|\hat{T}_1|$ reduces to

$$|\hat{T}_1| \approx \frac{\omega F}{70} \times \sqrt{\frac{1}{(\lambda + \epsilon\gamma)^2 + c^2\omega^2}}. \tag{9}$$

At these time-scales the deep ocean has not warmed up substantially ($T_2 \approx 0$), and uncertainties in λ, c, ϵ and γ all make substantial contributions to the total uncertainty in $|\hat{T}_1|$. However, because λ, ϵ, γ and c are all in the denominator, their uncertainties compensate, such that F is generally the largest contributor to uncertainty. Even if λ were zero, for instance, the warming at these frequencies would be finite, though the ECS would be infinite. The exception is very high frequencies, when small differences in c can result in large changes in $|\hat{T}_1|$.

We then define a fast time-scale as $\omega_H = (\lambda + \epsilon\gamma)/c$ (or $P_H = c/(\lambda + \epsilon\gamma)$), so that the effect of the mixed-layer heat capacity is negligible for $\omega_L << \omega < \omega_H$. In other words, it is only at frequencies higher than ω_H that uncertainties in c have a substantial impact on uncertainty in $|\hat{T}|$. The period P_H corresponds to the time-scale on which the upper ocean box equilibrates in the absence of warming of the deep ocean ($\frac{dT_1}{dt} \approx 0$ and $T_2 \approx 0$). So ω_H separates the ultra-high frequency ($\omega > \omega_H$, or $t < P_H$) regime from the high frequency regime ($\omega_L << \omega < \omega_H$, or $P_L >> t > P_H$).

As ω starts to approach ω_L, the approximation in equation 9 is no longer accurate, as there is warming of the deep ocean ($T_2 > 0$). In this intermediate frequency regime equation 8 can be approximated as

$$|\hat{T}_1| \approx \frac{\omega F}{70} \times \sqrt{\frac{1}{\left[\lambda + \epsilon\gamma\left(1 - \frac{\gamma^2}{\gamma^2 + c_0^2\omega^2}\right)\right]^2 + c_0^2\omega^2\epsilon^2/(\gamma^2 + c_0^2\omega^2)^2}}. \tag{10}$$

The $c_0\omega$ term is now key: as frequency decreases, this term gets smaller, so that $1 - \frac{\gamma^2}{\gamma^2 + c_0^2\omega^2}$ goes to zero, as does the last term in the denominator. Thus the contributions of ϵ and γ decrease with frequency in this regime.

Finally, on long time-scales ($\omega < \omega_L$, or $P > P_L$), after the deep ocean has equilibrated with the surface mixed layer ($T_1 \approx T_2$), the contributions of the ocean heat uptake terms, γ and ϵ, are negligible, and uncertainty in $\hat{T}_1$ is mostly determined by F and λ, as for the ECS:

$$|\hat{T}_1| \approx \frac{F}{\lambda}. \tag{11}$$

In summary, equation 8 can be used to separate transient warming into four regimes: the ultra-high frequency regime ($\omega > \omega_H$), the high frequency regime ($\omega_H > \omega >> \omega_L$), the intermediate frequency regime ($\omega \sim \omega_L$) and the low frequency regime ($\omega_L > \omega$). ω_H separates the ultra-high frequency and high frequency regimes, while the transition between the high frequency and intermediate frequency regimes occurs once there has been substantial warming of the deep ocean. Using the CMIP5 ensemble-mean values (see following section and Supplemental Table 2) gives $\omega_H \sim 4$ years^{-1} and $\omega_L \sim 160$ years^{-1}. Furthermore, defining "substantial warming" of the deep ocean as occurring when $\gamma \sim 0.1 c_0 \omega$ gives a time-scale of 16 years separating the high frequency and intermediate frequency regimes.

Working in frequency space also makes clear the differences in the contributions of ϵ and γ. In equations 9 and 10, ϵ always damps $|\hat{T}_1|$, so that larger ϵ results in smaller $|\hat{T}_1|$ at all frequencies. However, while larger γ makes $\epsilon\gamma$ larger, damping the warming, it also makes the terms $1 - \frac{\gamma^2}{\gamma^2 + c_0^2\omega^2}$ and $c_0^2\omega^2\epsilon^2/(\gamma^2 + c_0^2\omega^2)^2$ smaller, enhancing the warming. So the rate of ocean heat uptake acts as both a positive feedback and a negative feedback on transient temperature increases, and we can expect uncertainty in ϵ, which always damps temperature increases, to contribute more to uncertainty in $|\hat{T}_1|$ than uncertainty in γ.

These regimes are closely related to the "single-layer", "zero-layer" and "two-layer" regimes identified by *Gregory et al.* [2015]. In the single-layer regime there is no warming of the deep ocean, and the upper layer has not equilibrated with the forcing ($T_2 = 0$ and $dT_1/dt \neq 0$), so that equations 2 and 3 reduce to a single equation:

$$c\frac{dT_1(t)}{dt} \approx \Delta F(t) - (\lambda + \epsilon\gamma)T_1(t), \qquad \text{single-layer}, \tag{12}$$

In the zero-layer regime the upper layer has equilibrated and the deep ocean has still not experienced warming ($T_2 = 0$ and $dT_1/dt = 0$), so that equation 12 becomes

$$0 \approx \Delta F(t) - (\lambda + \epsilon\gamma)T_1(t), \qquad \text{zero-layer}. \tag{13}$$

These two regimes correspond to our ultra-high frequency and high frequency regimes, with the boundary between them again determined by the frequency ω_H. Finally, Gregory et al.'s two-layer regime includes warming of the deep ocean, assuming that the surface mixed-layer equilibrates much faster than the deep ocean so that $dT_1/dt = 0$:

$$0 \approx \Delta F(t) - \lambda T_1(t) - \epsilon\gamma(T_1(t) - T_2(t)), \qquad \text{double-layer}. \tag{14}$$

Our low frequency regime is obtained at the time-scales on which the surface mixed-layer and the deep ocean have roughly equilibrated ($T_1 \approx T_2$), so that equation 14 reduces to $\Delta F = \lambda T_1$.

Comparing the single-layer and zero-layer cases again shows that the dependence on c drops out on intermediate time-scales. Furthermore, except for the equilibrated state, when $T_1 = T_2$, the "climate resistance" ($\lambda+\epsilon\gamma$, *Gregory and Forster* [2008]) is non-zero because of heat transfer to the deep ocean, and so T_1 is less sensitive to λ than to F. However these approximations do not make clear the ambiguous dependence of T_1 on γ, nor the differing contributions of γ and ϵ.

3 CMIP5 Data Analysis

To make the contributions of the different factors to uncertainty in transient warming quantitative, we have fit equations 2 and 3 to simulations with 18 climate models participating in the fifth Climate Model Intercomparison Project (CMIP5), following the two-step procedure of *Geoffroy et al.* [2013a] (see Supplemental Text 1 and Supplemental Table 2). The relative uncertainty in each parameter, here defined as the standard deviation of the intermodel spread divided by the ensemble-mean, is shown in Figure 1a. The largest relative uncertainty is in c_0, followed by λ and then γ, ϵ, F and finally c. We note that correlations between the variables are generally weak, except for λ and λ, which have an r^2 value of 0.37 (Supplemental Table 3).

The distributions for the parameters from the fits can be used to analyze the sensitivity of transient warming, quantified by the TCR, to uncertainty in each parameter, allowing us to identify the main sources of uncertainty in transient warming and, more importantly, to interrogate the sensitivity of transient warming to uncertainty in each parameter. To do this, we performed a number of integrations with the EBM in which CO_2 concentrations are increased at 1% per year for 140 years. In each integration, the parameters were fixed at their ensemble means, except for one parameter, x, which was set to either $\bar{x}$, $\bar{x} + std(x)$, $\bar{x} - std(x)$, $\bar{x} + 2std(x)$, or $\bar{x} - 2std(x)$; where the overbars denote ensemble means and $std(x)$ is the standard deviation of x across the ensemble. With six parameters for x, this made 25 integrations in total, and we thus mapped out the sensitivity of the TCR to uncertainty in each parameter, assuming that the uncertainty in each parameter is normally distributed. In other words, we used these integrations to approximate the functions $\mathrm{TCR}'_x = f(x')$, where $'$ denotes an uncertainty and $x \in \{F, \lambda, \gamma, \epsilon, c, c_0\}$.

The results of these integrations, shown in Figure 1b, demonstrate that the net radiative feedback λ produces the largest range of TCR values, followed by the forcing F. Uncertainty in the rate of ocean heat uptake γ and the ocean heat uptake efficacy ϵ also contribute a substantial amount of spread, while the contributions of the heat capacities are negligible, despite the large relative uncertainty in c_0. However, this analysis combines the two components of uncertainty – the uncertainty in each parameter and the sensitivity of T_1 to each parameter. For example, the relative uncertainty in λ is nearly three times as large as the relative uncertainty in F (~32% compared to ~12%), yet the contribution of F to the uncertainty in the TCR is almost as large as that of λ. Thus in order to investigate the sensitivity of T_1 to uncertainty in each parameter, the EBM integrations were repeated assuming that all the parameters have the same relative uncertainty as λ. That is, the standard deviation of each of the other five distributions was set equal to 0.32 times the mean of the distribution, so that x' is the same for all x. This new analysis reveals that the TCR is twice as sensitive to uncertainty in F as it is to uncertainty in λ (Figure 1c). The other parameters are generally similar to before.

So although the net radiative feedback λ is the largest source of uncertainty in the TCR, this is only because the relative uncertainty in λ is three times as large as the relative uncertainty in F. Agreeing with the analysis in the previous section, the EBM integrations again demonstrate that the TCR is more sensitive to uncertainty in the forcing than to uncertainty in the feedbacks, so that a small reduction in the uncertainty of F is equivalent to a much larger reduction in the uncertainty of λ. Put another way, if the uncertainty in F were as large as the uncertainty in λ the spread in TCR across models would be ~0.5-3.5K, instead of 1-2.5K. We also note that the TCR's sensitivity to ϵ is larger than its sensitivity to γ, though both are smaller than the sensitivity to the feedback parameter.

Taking this further, Figure 2 shows the ratio of the sensitivity of T_1 to uncertainty in each of the parameters apart from F divided by the sensitivity of T_1 to uncertainty in F, as a function of time. Ratios smaller (larger) than one indicate that the sensitivity of T_1 at time t to F is larger (smaller) than to the other considered quantity. The sensitivity to λ increases with time relative to the sensitivity to F (dotted line), but even after 140 years the ratio is less than 0.8. It is only when the system has fully equilibrated – when T_1 = ECS – that the sensitivity to λ is the same as to F. The sensitivities to γ and ϵ decrease after about 20 years, approximately equal to the time-scale estimated in the previous section for when the deep ocean begins to warm. The sensitivity to ϵ is larger than the sensitivity to γ in this regime because of the opposing effects of γ on the temperature increase, a discussed in the previous section.

T_1 is highly sensitive to the value of c for the first ten years, when ωc is large, but after this the contribution of uncertainty in c is negligible.

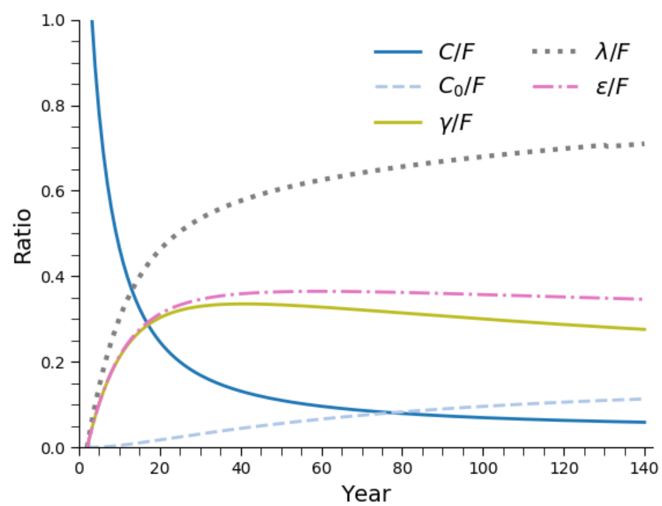

Figure 2. Ratio of sensitivity of T_1 to uncertainty in C to the sensitivity of T_1 to uncertainty in F as a function of time (solid blue line), ratio of sensitivity to C_0 to sensitivity to F (dashed blue line), ratio of sensitivity to γ to sensitivity to F (solid yellow line), ratio of sensitivity to λ to sensitivity to F (dotted gray line) and the ratio of sensitivity to ϵ to sensitivity to F (dot-dash pink line). These sensitivities are calculated from the EBM calculations assuming the same relative uncertainty in each parameter.

4 Implications

A first implication of this strong sensitivity of transient warming to F is that the most efficient way of narrowing the uncertainty in the TCR is developing better constraints on the raw radiative perturbation due to doubling atmospheric CO_2 concentrations (*Collins et al.* [2006]; *Soden et al.* [2018]), as well as on the rapid adjustments of the stratosphere and the troposphere which occur once CO_2 concentrations are increased and that are included in F (*Gregory and Webb* [2008]; *Zelinka et al.* [2013]; *Sherwood et al.* [2015]).

There are at least three additional implications of the strong sensitivity of transient warming to the radiative forcing. First, it implies a strong sensitivity of transient warming to the rate at which atmospheric CO_2 concentrations increase, since $\Delta F = F\ln(C/C_0)$. The time-evolution of CO_2 concentrations is determined by a combination of the rate at which carbon is emitted to the atmosphere and the carbon-cycle processes which control how efficiently carbon is removed from the atmosphere:

$$C(t) = \alpha(t) \times E(t), \tag{15}$$

where E is the emission of carbon to the atmosphere in a given year and α is the fraction of the emission which stays in the atmosphere. Hence even if the radiative forcing of doubling CO_2 concentrations were perfectly known, uncertainties in the emission scenario and/or in the carbon-cycle feedbacks could overwhelm uncertainties in λ when making predictions of T_1. Moreover, uncertainty in future aerosol forcing and in the forcings due to other greenhouse gases also contribute to uncertainty in the future radiative forcing. We note, however, that recent studies with earth system models suggest that the transient climate response to cumulative carbon emissions (TCRE = T_1/E) is more sensitive to uncertainties in physical climate properties (F, λ, etc.) than to uncertainties in carbon cycle processes, implying that the uncertainty in α across models is small (*Gillett et al.* [2013]; *Williams et al.* [2017]).

Second, the time-scale dependence of the climate system's warming, or cooling, suggests caution when extrapolating from short-lived climate perturbations, such as volcanic eruptions, to long-term perturbations. The response to the former is mostly determined by the upper ocean heat capacity and the forcing, so that a climate model's skill in fitting such a perturbation is primarily due to its estimates of c and F (and we note the additional complication of forcings having different efficacies [*Marvel et al.*, 2015]). Thus estimates of λ or of either of the ocean heat uptake parameters from a short-lived perturbation will reflect the estimates of c and F, and are unlikely to be representative of the climate system's response to long-term perturbations.

Finally, our results imply that uncertainties in the forcing can strongly affect attempts to tune climate models by fitting to the historical temperature record [*Voosen*, 2016]. By "tuning" we mean both cases in which model parameters are explicitly tweaked to better fit the 20th century temperature record and cases in which a particular model is deemed to be of low quality because it does not fit the record well. We illustrate this through simulations of the 20th century with the two-box model, forcing it with an estimate of the total radiative forcing over the 20th century, ΔF (see Supplementary Text). We then vary the forcing by up to ±1 standard deviation of the CO_2 forcing F. That is, we set $\Delta F' = \Delta F + \beta std(F)$, where β is varied from -1 to 1 in increments of 0.1 (see Supplementary Text S2 and Figure 3a). For each forcing assumption, we set c, c_0, γ and ϵ to their ensemble-mean values and perform simulations in which λ is varied in increments of $0.01\mathrm{Wm}^{-2}\mathrm{K}^{-1}$, searching for the value that gives the best fit to the 20th century temperature record for the forcing estimate. Figure 3b shows how the optimal value of λ varies as a function of ΔF at the end of the 20th century in these simulations (circles), with a linear least-squares regression indicating that a 1% change in the estimate of the net forcing resulting in a 1.88% change in the optimal value of λ.

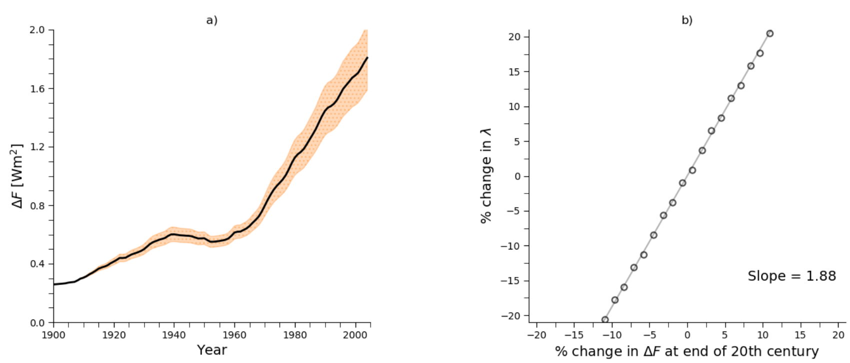

Figure 3. a) Net historical radiative forcing ΔF for the period 1900 to 2005 (black line) and estimates of ΔF with the CO_2 forcing varied by up to ± one standard deviation from the ensemble-mean for each species (orange shading). b) % change in the optimal value of λ as a function of the % change in ΔF (circles). The solid line shows a linear-least squares fit, with the slope indicated in the lower right of the panel. Note that the linearity does not hold for larger fractional changes in ΔF.

These calculations ignore, among other things, the different forcing efficacies of greenhouse gases (*Hansen et al.* [2005]; *Kummer and Dessler* [2014]; *Marvel et al.* [2015]), the question of the historical aerosol forcing [*Stevens*, 2015] and internal variability (*Silvers et al.* [2018]; *Andrews et al.* [2018]), but demonstrate the strong sensitivity of radiative feedbacks in models that are tuned by fitting to the historical temperature record to assumptions made about the forcing over the 20th century. If the same model were tuned twice using historical forcing estimates that differed by 20%, the resulting values of λ would differ by 38%.

5 Conclusion

Using a combination of theory and analysis of data from the CMIP5 archive, we have shown here that transient warming, typically represented by the TCR or T140, is most sensitive to uncertainty in F, the radiative forcing from doubling CO_2 concentrations, followed by uncertainty in the radiative feedbacks λ. This contrasts with the equilibrated warming (ECS), which is equally sensitive to uncertainty in F and in λ^{-1}. This difference reflects the role of ocean heat uptake in transient warming, as even if λ were zero the TCR would still be finite because of heat transfer to the deep ocean, whereas the ECS would be undefined. Our analysis has also shown that transient warming is more sensitive to the efficacy of ocean heat uptake (ϵ) than the rate of ocean heat uptake (γ), though the contributions of both of these to uncertainty in transient warming decreases after about 20 years.

These results suggest that more emphasis should be placed on constraining the uncertainty in F, as well as on constraining the historical forcing, as small changes in the assumed historical forcing can have large impacts on the radiative feedbacks in climate models that are tuned using historical data. Furthermore, the sensitivity to F can also be taken to be a sensitivity to the carbon cycle feedbacks which convert CO_2 emissions to atmospheric CO_2 concentrations. Even if the radiative forcing of doubling CO_2 concentrations were perfectly known, uncertainties in the emission scenario and/or in the carbon-cycle feedbacks could overwhelm uncertainties in λ.

As has been recently noted, uncertainty in F could be substantially reduced if the number of radiative transfer parameterizations used in climate models was reduced, so that only parameterizations that have been thoroughly vetted against line-by-line calculations were implemented in climate models [*Soden et al.*, 2018]. Our results emphasize the urgency of this consolidation, as well as the importance of better constraining the rapid adjustments which take place as soon as CO_2 concentrations are increased (particularly in the stratosphere [*Chung and Soden*, 2015]), better constraining the carbon-cycle feedbacks which determine how efficiently carbon is removed from the atmosphere, and better constraining the historical forcing, for which much of the uncertainty comes from uncertainty in the radiative effects of aerosols in the late 19th and early 20th centuries [*Stevens*, 2015].

Climate models are increasingly including representations of the aerosol indirect effect, which can make their estimates of the historical aerosol forcing larger (i.e., more negative; see e.g., *Carslaw et al.* [2013]; *Nazarenko et al.* [2017]), and thus an increase in the spread in the modelled historical aerosol forcing across the next generation of CMIP models can be expected. Our analysis suggests an approximate 2:1 relationship between uncertainty in climate models' net radiative feedback and uncertainty in the historical forcing, implying that the increased spread in models' estimate of the historical aerosol forcing will substantially increase the model spread in radiative feedbacks.

Acknowledgments

We thank Daniel Koll, Susan Solomon, Thorsten Mauritsen, Isaac Held and Gillian Shaffer for helpful discussions and comments on earlier versions of this manuscript. N.J.L. was supported by the NSF through grant AGS-1623218, "Collaborative Research: Using a Hierarchy of Models to Constrain the Temperature Dependence of Climate Sensitivity". The data and scripts used in section 3 are available at: https://github.com/nicklutsko/TCR_Uncertainty/.

References

Andrews, T., J. M. Gregory, D. Paynter, L. G. Silvers, C. Zhou, T. Mauritsen, M. J. Webb, K. C. Armour, P. M. Forster, and H. Titchner (2018), Accounting for changing temperature patterns increases historical estimates of climate sensitivity, *Geophysical Research Letters*, *45*, 8490–8499.

Carslaw, K.-S., L. A. Lee, C. L. Reddington, K. J. Pringle, A. Rap, P. M. Forster, G. W. Mann, D. V. Spracklen, M. T. Woodhouse, L. A. Regayre and J. R. Pierce (2013), Large contribution of natural aerosols to uncertainty in indirect forcing, *Nature*, *503*, 67-71.

Chung, E.-S., and B. J. Soden (2015), An assessment of methods for computing radiative forcing in climate models, *Environmental Research Letters*, *10*(6), 074,004.

Collins, W. D., V. Ramaswamy, M. D. Schwarzkopf, Y. Sun, R. W. Portmann, Q. Fu, S. E. B. Casanova, J.-L. Dufresne, D. W. Fillmore, P. M. D. Forster, V. Y. Galin, L. K. Gohar, W. J. Ingram, D. P. Kratz, M.-P. Lefebvre, J. Li, P. Marquet, V. Oinas, Y. Tsushima, T. Uchiyama, and W. Y. Zhong (2006), Radiative forcing by well-mixed greenhouse gases: Estimates from climate models in the intergovernmental panel on climate change (ipcc) fourth assessment report (ar4), *Journal of Geophysical Research: Atmospheres*, *111*(D14).

Dufresne, J., and S. Bony (2008), An assessment of the primary sources of spread of global warming estimates from coupled atmosphere-ocean models., *Journal of the Atmospheric Sciences*, *21*(24), 5135–5144.

Etminan, M., G. Myhre, E. J. Highwood, and K. P. Shine (2016), Radiative forcing of carbon dioxide, methane, and nitrous oxide: A significant revision of the methane radiative forcing, *Geophysical Research Letters*, *43*(24), 12,614–12,623.

Geoffroy, O., D. Saint-Martin, and A. Ribes (2012), Quantifying the sources of spread in climate change experiments., *Geophysical Research Letters*, *39*(24), L24,703.

Geoffroy, O., D. Saint-Martin, G. Bellon, A. Voldoire, D. J. L. Olivie, and S. Tyteca (2013a), Transient climate response in a two-layer energy-balance model. part i: Analytical solution and parameter calibration using cmip5 aogcm experiments, *Journal of Climate*, *26*(6), 1841–1859.

Geoffroy, O., D. Saint-Martin, G. Bellon, A. Voldoire, D. J. L. Olivie, and S. Tyteca (2013b), Transient climate response in a two-layer energy-balance model. part ii: Representation of the efficacy of deep-ocean heat uptake and validation for cmip5 aogcms, *Journal of Climate*, *26*(6), 1859–1876.

Gillett, N. P., V. K. Arora, D. Matthews, and M. R. Allen (2013), Constraining the ratio of global warming to cumulative co2 emissions using cmip5 simulations, *Journal of Climate*, *26*(20), 6844–6858.

Gregory, J. M. (2000), Vertical heat transports in the ocean and their effect on time-dependent climate change, *Climate Dynamics*, *16*(6), 501–515.

Gregory, J. M., and P. M. Forster (2008), Tropospheric adjustment induces a cloud component in co2 forcing, *Journal of Geophysical Research: Atmospheres*, *113*(9), d23105.

Gregory, J. M., and M. Webb (2008), Tropospheric adjustment induces a cloud component in co2 forcing, *Journal of Climate*, *21*, 58–71.

Gregory, J. M., T. Andrews, and P. Good (2015), The inconstancy of the transient climate response parameter under increasing COâĆĆ, *Philosophical Transactions of the Royal Society of London*, *373*, 20140417.

Grose, M. R., J. M. Gregory, R. Colman, and T. Andrews,What Climate Sensitivity Index Is Most Useful for Projections?, *Geophysical Research Letters*, *45*, 1559âĂŞ 1566.

Hamby, D. M. (1994), A review of techniques for parameter sensitivity analysis of environmental models, *Environmental Monitoring and Assessment*, *32*(2), 135–154.

Hansen, J., M. Sato, R. Ruedy, L. Nazarenko, A. Lacis, G. A. Schmidt, G. Russell, I. Aleinov, M. Bauer, S. Bauer, N. Bell, B. Cairns, V. Canuto, M. Chandler, Y. Cheng, A. Del Genio, G. Faluvegi, E. Fleming, A. Friend, T. Hall, C. Jackman, M. Kelley, N. Y. Kiang, D. Koch, J. Lean, J. Lerner, K. Lo, S. Menon, R. L. Miller, P. Minnis, T. Novakov, V. Oinas, J. P. Perlwitz, J. Perlwitz, D. Rind, A. Romanou, D. Shindell, P. Stone, S. Sun, N. Tausnev, D. Thresher, B. Wielicki, T. Wong, M. Yao, and S. Zhang (2005), Efficacy of climate forcings, *J. Geophys. Res.*, *110*, D18,104.

Held, I. M., M. Winton, K. Takahashi, T. Delworth, F. Zeng, and G. K. Vallis (2010), Probing the fast and slow components of global warming by returning abruptly to preindustrial forcing, *Journal of Climate*, *23*(6), 2418–2427.

Kummer, J. R., and A. R. Dessler (2014), The impact of forcing efficacy on the equilibrium climate sensitivity., *Geophysical Research Letters*, *41*(2), 3565–3568.

Marvel, K., G. A. Schmidt, R. L. Miller, and L. S. Nazarenko (2015), Implications for climate sensitivity from the response to individual forcings., *Nature Climate Change*, *6*(2), 386–389.

Myhre, G., E. J. Highwood, K. P. Shine, and F. Stordal (1998), New estimates of radiative forcing due to well mixed greenhouse gases, *Geophysical Research Letters*, *25*(14), 2715–2718.

Nazarenko, L., D. Rind, K. Tsigaridis, A. D. Del Genio, M. Kelley and N. Tausnev (2017), Interactive nature of climate change and aerosol forcing, *Geophysical Research Letters*, *122*(14), 3457–3480.

Sherwood, S. C., S. Bony, O. Boucher, C. Bretherton, P. M. Forster, J. M. Gregory, and B. Stevens (2015), Adjustments in the forcing-feedback framework for understanding climate change, *Bulletin of the American Meteorological Society*, *96*(6), 217–228.

Silvers, L. G., D. Paynter, and M. Zhao (2018), The diversity of cloud responses to twentieth century sea surface temperatures, *Geophysical Research Letters*, *45*(1), 391–400, 2017GL075583.

Soden, B. J., W. D. Collins, and D. R. Feldman (2018), Reducing uncertainties in climate models, *Science*, *27*, 326–327.

Stevens, B. (2015), Rethinking the lower bound on aerosol radiative forcing, *Journal of Climate*, *28*(2), 4794–4819.

Stocker, T. F. e. a. (Ed.) (2013), *IPCC Climate Change 2013: The Physical Science Basis*, 1 ed., Cambridge University Press.

Voosen, P. (2016), Climate scientists open up their black boxes to scrutiny, *Science*, *28*, 401–402.

Williams, R. G., V. Roussenov, P. Goodwin, L. Resplandy, and L. Bopp (2017), Sensitivity of global warming to carbon emissions: Effects of heat and carbon uptake in a suite of earth system models, *Journal of Climate*, *30*(20), 9343–9363.

Winton, M., K. Takahashi, and I. M. Held (2010), Importance of ocean heat uptake efficacy to transient climate change, *Journal of Climate*, *23*(6), 2333–2344.

Zelinka, M. D., S. A. Klein, and K. E. Taylor (2013), Contributions of different cloud types to feedbacks and rapid adjustments in cmip5, *Journal of Climate*, *26*, 5007–5027.